Article

Generalized Thrust Network Analysis of Triangular Masonry Cross Vaults Inspired by Musmeci

Nicola A. Nodargi * , **Claudio Intrigila** and **Paolo Bisegna**

Department of Civil Engineering and Computer Science, University of Rome Tor Vergata, 00133 Rome, Italy; intrigila@ing.uniroma2.it (C.I.); bisegna@uniroma2.it (P.B.)
* Correspondence: nodargi@ing.uniroma2.it

Abstract: A triangular parabolic cross vault, that was designed by Musmeci in the 1950s as a reinforced concrete structure but remained unbuilt, is revisited from the original perspective of its reinvention as a masonry structure. In the framework of static limit analysis under classical Heyman's assumptions, a generalized thrust network analysis is adopted for a structural safety assessment. The performances of the vault, subject to its self-weight, are investigated through minimum-thrust and minimum-thickness analyses by conforming to the original geometry and assuming the vault thickness as the only design parameter. Further insight is achieved by exploring a more general class of triangular parabolic masonry cross vaults, whose rise-to-span ratio is an additional design parameter. The static efficiency of the smart and unconventional geometry proposed by Musmeci is thus proven, motivating the possibility of bringing it to new life in the form of a masonry structure.

Keywords: historical monuments; masonry; cross vaults; limit analysis; thrust network analysis; minimum thrust; minimum thickness; geometric safety factor; structural optimization; linear programming

1. Introduction

In 1954, the Italian engineer Sergio Musmeci (1926–1981) designed a reinforced concrete cross vault, characterized by a triangular layout and obtained by assembling three triangular webs with parabolic profiles [1]. Although the vault geometry was a unique and pioneering result of structural optimization, it remained unbuilt and its project was only mentioned in reference [2] as "exemplary for its modular conception of the structure based on the repetition of cylindrical shells".

The smart geometry invented by Musmeci is revisited here to explore its potential realization as a masonry structure, as first proposed in references [3,4], and it is then taken for inspiration in considering the design of a more general class of triangular masonry cross vaults. As a reliable structural assessment methodology of masonry vaults, the static (or safe) theorem of limit analysis is adopted, following its formulation by Heyman under the assumptions of null tensile strength, infinite compressive strength, and no-sliding behavior [5–7].

Departing from the classical slicing technique (for a recent application, see, e.g., reference [8]), which models a typical masonry vault as a series of independent arch slices, thrust network analysis (TNA) has established itself as a powerful and automatic technique for the 3D funicular analysis of masonry vaults under gravitational loads [9,10]. It consists of finding a discrete network of compressive forces (or thrusts) in equilibrium with the vault self-weight, as reduced to nodal forces by tributary areas, and completely contained within the vault thickness. Peculiar to the method is the introduction of a form diagram, prescribing the network in horizontal projection and entailing a specific pattern of the internal force flow. Consequently, the unknown nodal heights and force densities

(i.e., the thrust-to-length ratios of the branches) are determined through a suitable nonlinear optimization problem enforcing nodal equilibrium equations and static admissibility conditions [11–17].

The TNA is mechanically interpreted by relating the network nodes to rigid masonry blocks ideally constituting the vault. Accordingly, the nodal equilibrium amounts to the equilibrium of the blocks under their self-weight and the interface forces, regarded as the thrusts in the network branches. In reference [18], Block observed that "the equilibrium of a masonry unit, or voussoir, in the vault does not require all forces to meet at one point in 3D space". In other words, the TNA assumption that all thrusts applied to a network node converge to that node is a sufficient, but not necessary, rotational equilibrium condition for the blocks. This observation has motivated the recent introduction of the generalized thrust network analysis (GTNA) [19]. Among its advantages, the GTNA allows an extension of the set of equilibrated and statically admissible stress states in the vault and translates the classical minimum-thrust problem for the safe assessment of the vault into a simple linear programming problem.

Besides the intrinsically discrete formulations discussed above, continuous methods have been proposed for the static limit analysis of masonry vaults. The thrust surface analysis approach describes the statics of a masonry vault by searching for a compressed thrust membrane within the vault thickness in equilibrium with its self-weight [20–24]. A generalization of that approach is offered by shell-based static limit analysis formulations, which overcome the thrust membrane concept by assuming that general shell stress states can arise within the vault to resist external actions [25–31]. Thrust surface analysis and shell-based static limit analysis can be regarded as the counterpart continuous methods of TNA and GTNA, respectively. A general and comprehensive review of computational methods for the structural analysis of masonry structures can be found in reference [32]. Experimental and computational investigations specifically devoted to the structural behavior of masonry cross vaults under diverse external actions have been discussed in, e.g., reference [33–35].

In the present paper, the GTNA is adopted for investigating the structural safety of a masonry instance of the Musmeci vault. Initially, by conforming to the original geometry, the vault thickness is assumed as the only design parameter. Minimum-thrust and minimum-thickness analyses are performed, respectively enlightening the potential stress states in the vault after outward settlements of the supports and the geometric safety factor of the structure, as defined in reference [5]. Subsequently, the Musmeci vault is regarded as representative of a class of triangular parabolic masonry cross vaults parameterized by their rise-to-span ratio and normalized thickness. Minimum-thrust and minimum-thickness analyses are thus extended through parametric analyses, informing of the structural behavior of such unconventional structures.

The paper is organized as follows. In Section 2, the Musmeci structural model is reviewed. In Section 3, the fundamentals of GTNA are discussed. In Section 4, the minimum-thrust and minimum-thickness analyses of the Musmeci vault as a masonry structure are presented. Their extension to a parametric class of triangular parabolic masonry cross vaults is carried out in Section 5. The conclusions are outlined in Section 6.

2. Musmeci Triangular Parabolic Cross Vault

The structure referred to here as the Musmeci vault consists of a reinforced concrete parabolic cross vault with an equilateral triangular bay. It was conceived by Sergio Musmeci, in collaboration with the architect Giuseppe Vaccaro, in 1954, as a module forming, through four-fold repetition, the cover of a rural market in southern Italy [1,2]. The cover, which accommodated the rhomboidal layout of the market space, was the result of Musmeci's early investigations on structural design optimization. An original sketch of the planar view and a reconstructed perspective view of the whole structure are depicted in Figure 1. In detail, each vault was formed by three triangular webs with parabolic profile, characterized by external arches with a rise $f = 3.65\,\text{m}$ and span $2a = 12.50\,\text{m}$. The intersection of

the three webs generated the ribs of the vault as semi-parabolic arches with a rise f and span $b = a/\cos(30°) = 2a/\sqrt{3} = 7.22\,\mathrm{m}$. In the following, the equilibrium design approach developed within the original Musmeci structural model [1] is briefly described, as also reviewed in references [3,4].

(a)   (b)
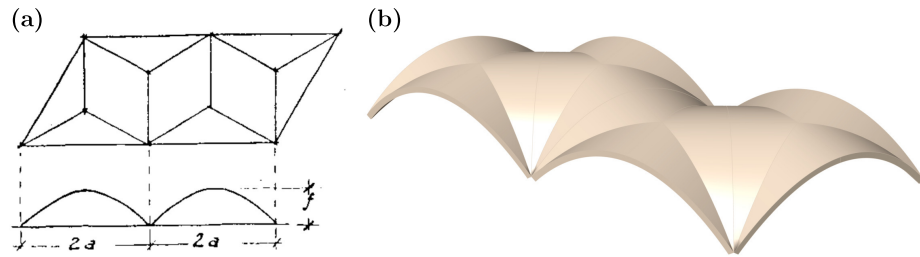
Figure 1. Musmeci triangular parabolic cross vault: (**a**) original sketch of the planar view, reproduced from reference [1], and (**b**) reconstructed three-dimensional view.

For the typical triangular vault to be considered, the Cartesian reference frame shown in Figure 2 is introduced. A slicing technique is adopted to find an equilibrated membrane stress state in the parabolic webs. By using a symmetry argument, only the web whose ridge line is parallel to the y-axis is considered. It is discretized into a family of independent parabolic web arches of infinitesimal width $\mathrm{d}y$, with a span linearly increasing from 0 to $2a$, and with mid-curve parameterized as follows:

$$z(x) = \frac{f}{a^2}x^2. \tag{1}$$
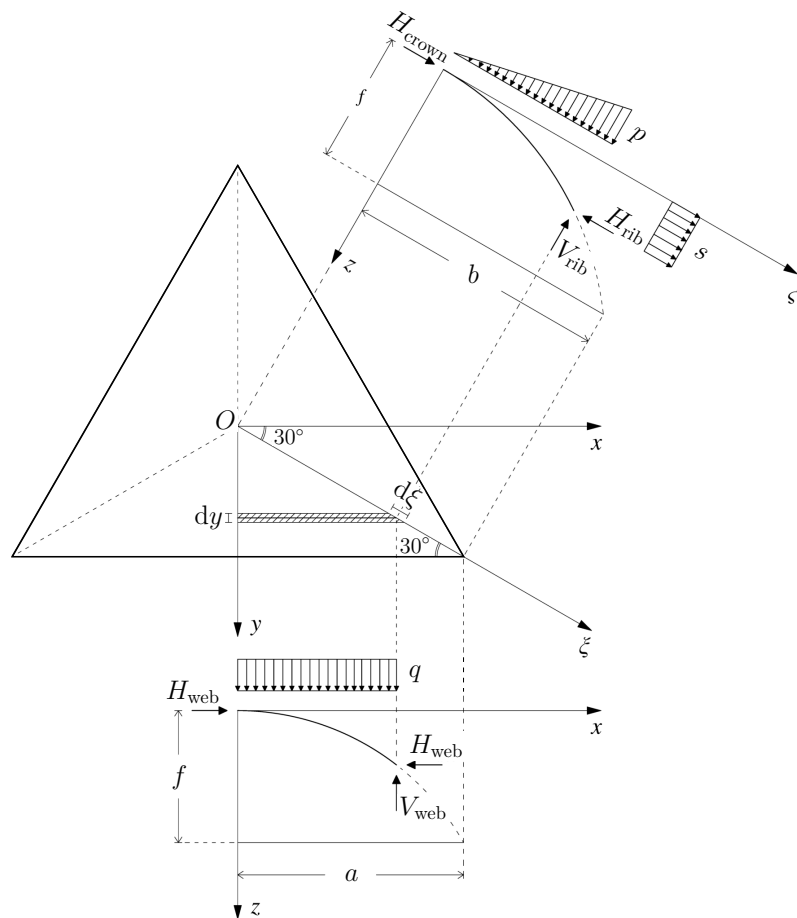
Figure 2. Musmeci triangular parabolic cross vault: structural model [4].

Motivated by the web shallowness, the web self-weight is assumed to be approximately uniform in horizontal projection and with a magnitude q per unit surface. It follows that the vertical and horizontal actions (per unit $\mathrm{d}y$ in horizontal projection) transmitted by the web arch of span $2x$ to the rib arch are, respectively, given by:

$$V_{\text{web}}(x) = qx, \quad H_{\text{web}} = \frac{qa^2}{2f}. \tag{2}$$

Consequently, the rib arch, which is parameterized in terms of the abscissa $\xi = x/\cos(30°) = 2x/\sqrt{3}$ as

$$z(\xi) = \frac{f}{b^2}\xi^2, \tag{3}$$

is subjected to the vertical and horizontal loads (per unit $\mathrm{d}\xi$ in horizontal projection), respectively, given by:

$$p(\xi) = 2V_{\text{web}}(x(\xi))\frac{\mathrm{d}y}{\mathrm{d}\xi} = \frac{\sqrt{3}}{2}q\xi, \quad s(\xi) = 2H_{\text{web}}\cos(30°)\frac{\mathrm{d}y}{\mathrm{d}\xi} = \frac{3\sqrt{3}}{16}\frac{qb^2}{f}. \tag{4}$$

Since the rib is subjected to a vertical load p linearly varying from the crown to the abutment, Musmeci inferred that the thrust line differs from the parabolic rib mid-curve. However, he realized that the constant horizontal load s was capable of bringing the former very close to the latter, the maximum eccentricity resulting in a few centimeters [1]. A structural analysis of the ribs was carried out by observing that, "Since the flexural stiffness of rib is practically negligible at the abutment, where the section is theoretically reduced to a point, and at the crown, where the angle between webs becomes zero, the behavior of the rib can be considered similar to that of a three-hinged semi-arch". On such a basis, the vertical reaction at the abutment is given by:

$$V = \int_0^b p(\xi)d\xi = \frac{\sqrt{3}}{4}qb^2 = \frac{\sqrt{3}}{3}qa^2, \tag{5}$$

the thrust follows from the rotational equilibrium about the crown hinge as

$$H = \frac{1}{f}\left(Vb - \int_0^b p(\xi)\xi d\xi + \int_0^b s(\xi)z(\xi)d\xi\right) = \frac{7\sqrt{3}}{48}\frac{qb^3}{f} = \frac{7}{18}\frac{qa^3}{f}, \tag{6}$$

and the thrust value at the crown results in

$$H_{\text{crown}} = H - \int_0^b s(\xi)d\xi = -\frac{\sqrt{3}}{24}\frac{qb^3}{f} = -\frac{qa^3}{9f}, \tag{7}$$

the negative sign implying that tensile stresses arise in the rib from the crown to the neutral point located at the abscissa $\xi = 2b/9 = 1.60\,\text{m}$. In particular, the normalized thrust at the abutment is estimated to be:

$$\frac{H}{V} = \frac{7}{6\sqrt{3}}\frac{a}{f} \approx 1.153. \tag{8}$$

The Musmeci project assumes the vault thickness to range from 12 to 8 cm (with tapering in the crown region), the ribs having a triangular section with a height of 28 cm. The webs are connected along the external sides by edge curbs recalling the *formeret* arches adopted in Gothic masonry vaults. The edge curbs have an almost rectangular section, with a thickness ranging from 15 to 22 cm. The reinforcement layout of the vault is shown in Figure 3. In detail, the whole surface of the webs is reinforced by a welded mesh with 6 cm pitch, whereas the edge curbs and the ribs are reinforced by 12 mm top and bottom longitudinal bars and 6 mm diameter stirrups with 20 cm pitch. It is observed that the arrangement of reinforcement bars along the ribs is consistent with their structural role of curved beams in the Musmeci model.
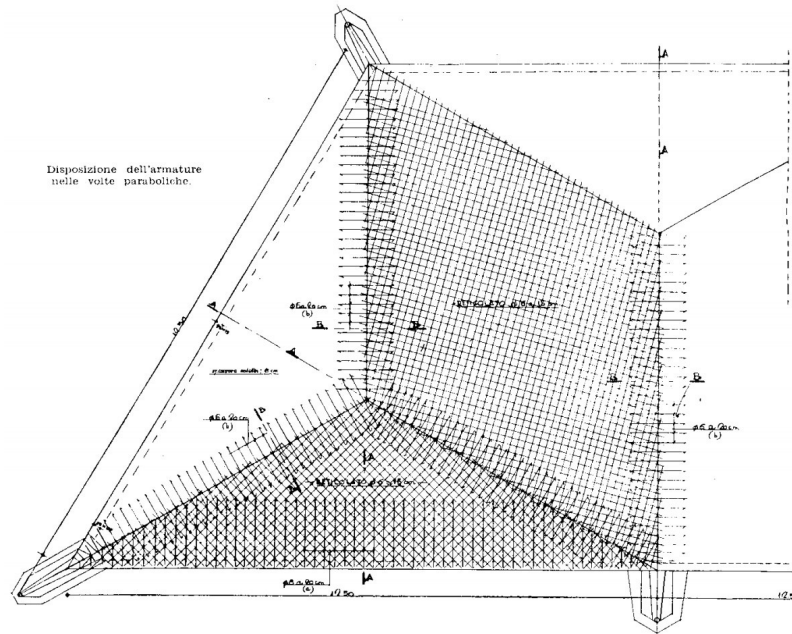
Figure 3. Musmeci triangular parabolic cross vault: reinforcement layout, reproduced from reference [1].

3. Generalized Thrust Network Analysis of Masonry Vaults

The possibility of reinventing the Musmeci triangular parabolic cross vault as a masonry vault is investigated here. To that aim, the safe assessment of a masonry instance of the vault is performed by adopting a generalized thrust network analysis (GTNA). A brief review of the method is presented in the following section (for further details, see reference [19]).

3.1. Discretization

The vault is discretized by considering a 3D network of B beams on its mid-surface (Figure 4). Consistently, the vault self-weight is concentrated at the network nodes according to their tributary areas. Let $(O; x, y, z)$ denote a Cartesian reference frame. The typical node n, of coordinates $x_n = (x_n; y_n; z_n)$, is subjected to external forces and couples denoted by $f_n = (f_{xn}; f_{yn}; f_{zn})$ and $m_n = (m_{xn}; m_{yn}; 0)$, respectively. In particular, it is assumed that no external couple is applied at the node about the z-axis. The vault thickness at the node, vertically measured, is decomposed as $h_n = h_n^{\text{ext}} + h_n^{\text{int}}$, with h_n^{ext} [resp., h_n^{int}] standing for the vertical distance of the node from the vault extrados [resp., intrados].

A local reference frame is associated with the typical beam b, given by the unit vectors:

$$t_{\text{H}}^b = \frac{1}{l_{\text{H}}^b} \begin{pmatrix} \Delta x^b \\ \Delta y^b \\ 0 \end{pmatrix}, \quad k = \begin{pmatrix} 0 \\ 0 \\ 1 \end{pmatrix}, \quad b^b = \frac{1}{l_{\text{H}}^b} \begin{pmatrix} -\Delta y^b \\ \Delta x^b \\ 0 \end{pmatrix}, \tag{9}$$

where Δx^b, Δy^b, and Δz^b are the coordinate differences between the beam end-sections. Specifically, t_{H}^b is parallel to the horizontal projection of the beam (whose length is l_{H}^b) and b^b is normal to the vertical plane π^b that contains the beam.
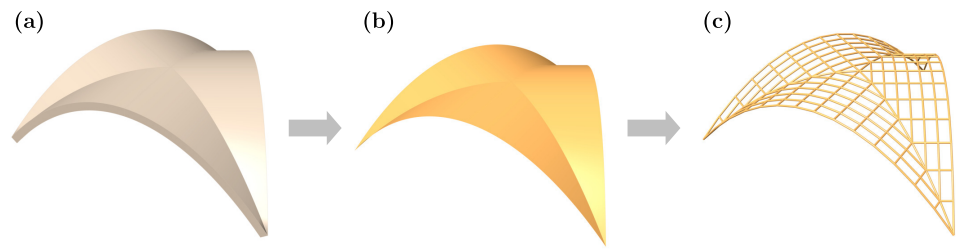
Figure 4. Generalized thrust network analysis of masonry vaults: geometric modeling of the Musmeci vault from (**a**) solid model, to (**b**) mid-surface, to (**c**) 3D beam networks.
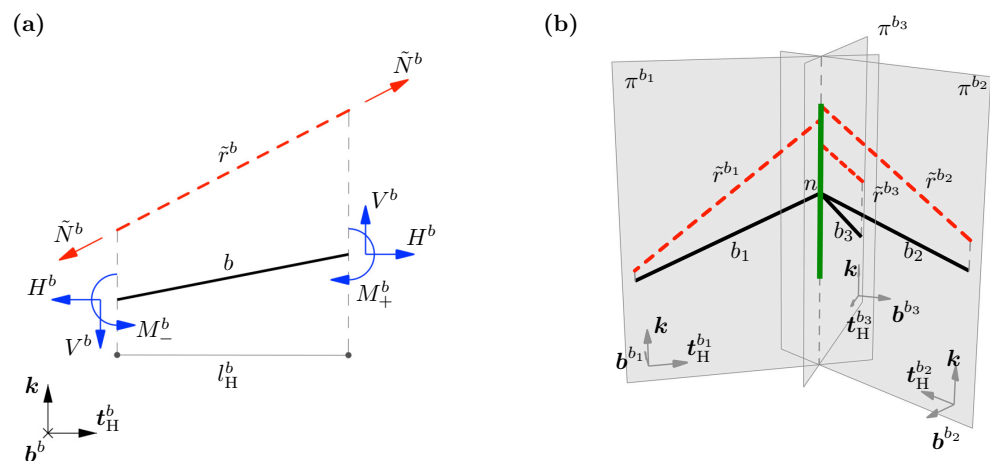
3.2. Stress State and Equilibrium

The typical network beam b is assumed to behave as an in-plane beam loaded in the vertical plane π^b. The following three statical descriptors are, therefore, introduced:

$$\boldsymbol{X}^b = \left(H^b; V^b; M^b \right), \tag{10}$$

representing the horizontal and vertical components of the internal resultant force, and the bending moment at the beam mid-section, respectively. For a visualization, it is observed that such a stress state is statically equivalent to a thrust force $\tilde{N}^b$ along a suitable straight line $\tilde{r}^b$ (Figure 5a). Accordingly, the beam equilibrium implies that the resultant forces $\pm \boldsymbol{R}_\pm$ and moments $\pm \boldsymbol{M}_\pm$ at the beam end-sections (with positive or negative sign prevailing for the initial or final section, respectively) are given by:

$$\begin{pmatrix} \boldsymbol{R}_\pm^b \\ \boldsymbol{M}_\pm^b \end{pmatrix} = \boldsymbol{E}_\pm^b \boldsymbol{X}^b, \quad \boldsymbol{E}_\pm^b = \begin{bmatrix} \boldsymbol{t}_H^b & \boldsymbol{k} & \boldsymbol{0} \\ \mp \dfrac{\Delta z^b}{2} \, \boldsymbol{b}^b & \pm \dfrac{l_H^b}{2} \, \boldsymbol{b}^b & \boldsymbol{b}^b \end{bmatrix}. \tag{11}$$

In passing, it is noted that, because $\boldsymbol{M}_\pm^b$ is parallel to $\boldsymbol{b}^b$, the matrices $\boldsymbol{E}_\pm^b$ have null entries in the last row.

Figure 5. Generalized thrust network analysis of masonry vaults: (**a**) stress state in the typical network beam and (**b**) equilibrium of the typical network node [19].

Accounting for the stress state in the network beams, the nodal equilibrium equations for the typical network node n result to be (Figure 5b):

$$\boldsymbol{E}_n \boldsymbol{X} + \boldsymbol{p}_n + \boldsymbol{r}_n = \boldsymbol{0}, \tag{12}$$

in which $\boldsymbol{X}$ is the $3B \times 1$ vector collecting the beam statical descriptors, $\boldsymbol{E}_n$ is the $6 \times 3B$ nodal equilibrium matrix constructed by standard assembling of the beam equilibrium

matrices $E_\pm^b$ in Equation (11), and $p_n = (f_n; m_n)$ and r_n, respectively, are the 6×1 vectors of nodal external loads and (possibly present) nodal constraint reactions. The presence of nodal constraint reactions r_n in Equation (12) is generally undesirable, for they involve a number of unknown parameters, collected into a vector λ_n, equal to the constraint multiplicity C_n. Conversely, it is preferable to reduce to the $(6 - C_n)$ pure equilibrium conditions:

$$\overline{E}_n X + \overline{p}_n = 0, \tag{13}$$

obtained by projecting the equilibrium Equation (12) along the unconstrained nodal degrees of freedom.

Upon column-stacking such equations for all the network nodes, the structural equilibrium equations are found:

$$E X + p = 0. \tag{14}$$

In closing, it is remarked that the assembling of the nodal rotational equilibrium equation about the z-axis can be avoided from the beginning, because it is identically satisfied for all the nodes (Figure 5b).

3.3. Static Admissibility

The classical Heyman's assumptions for masonry prescribe the vault to be compressed [5]. Within GTNA formulation, such an admissibility requirement is accounted for by restricting the stress state in the network beams. Specifically, for the typical beam b, it is enforced that:

$$H^b \leq 0, \quad M_\pm^b + H^b h_\pm^{\text{int}} \leq 0, \quad -M_\pm^b + H^b h_\pm^{\text{ext}} \leq 0, \tag{15}$$

where $h_\pm^{\text{int}}$ [resp., $h_\pm^{\text{ext}}$] denotes the vertical distance h_n^{int} from the vault intrados [resp., extrados] of the node n corresponding to the initial or beam end-section. Those conditions imply that the beam is compressed and the center of pressure at the beam end-sections is contained within the corresponding vertical sections of the vault. Requirement $(15)_1$ will be, henceforth, dropped off upon observing that it is linearly dependent on the two remaining conditions.

Using the relationships (10), the conditions (15) can be compactly written as follows:

$$A^b X^b \leq 0, \quad A^b = \begin{bmatrix} h_-^{\text{int}} + \dfrac{\Delta z^b}{2} & -\dfrac{l_{\text{H}}^b}{2} & 1 \\[2ex] h_-^{\text{ext}} - \dfrac{\Delta z^b}{2} & \dfrac{l_{\text{H}}^b}{2} & -1 \\[2ex] h_+^{\text{int}} - \dfrac{\Delta z^b}{2} & \dfrac{l_{\text{H}}^b}{2} & 1 \\[2ex] h_+^{\text{ext}} + \dfrac{\Delta z^b}{2} & -\dfrac{l_{\text{H}}^b}{2} & -1 \end{bmatrix}, \tag{16}$$

which, assembled for all the network beams, provide the structural admissibility conditions:

$$A X \leq 0, \tag{17}$$

with A as the $4B \times 3B$ structural admissibility matrix.

3.4. Structural Safety Assessment

A structural safety assessment of the vault is performed by the classical minimum-thrust and minimum-thickness problems (see, e.g., references [6,7]).

In the former problem, it is assumed that the vault supports undergo outward settlements, as generally caused by external loads. Consequently, the vault experiences a settlement mechanism which drives it into a minimum-thrust state. According to the

static theorem of the minimum thrust [7], such a stress state minimizes the opposite of the (resistant) work done by the settling constraints reactions:

$$\mathcal{W} = -\sum_{n \in \mathcal{C}} \delta_n^T \lambda_n = -\delta^T(WX + b), \tag{18}$$

where the $C_n \times 1$ vector δ_n collects the settlement parameters assigned for any constrained node $n \in \mathcal{C}$. The minimization is performed over the set of equilibrated and statically admissible stress states, amounting to the following optimization problem:

$$\begin{aligned} \min_{X} \quad & -\delta^T(WX + b), \\ \text{s.t.} \quad & EX + p = 0, \\ & AX \le 0. \end{aligned} \tag{19}$$

It is remarked that such a formulation consists of a linear programming problem and can be effectively addressed using standard optimization software. Details on the assembly procedure of δ, W, and b can be found in reference [19]. Therein, it has also been shown that, by interpreting the dual of the optimization problem (19) as a formulation of the kinematic theorem of the minimum thrust, the settlement mechanism of minimum thrust can be recovered by a simple post-computation. Needless to say, by changing the sign of δ, the maximum-thrust state in the vault can be explored instead of the minimum-thrust one.

The minimum-thickness problem offers a quantitative estimation of the structural safety of the vault under its self-weight in terms of the geometric safety factor [5]. Upon denoting as h the actual vault thickness and as $h_{\min}$ the minimum thickness for which the vault would be able to stand, the geometric safety factor is, in fact, given by the ratio $h/h_{\min}$. Here, a computational strategy based on the solution of a sequence of minimum-thrust analyses is adopted for determining the minimum thickness. The underlying idea is that a prescribed thickness h is safe only if the minimum thrust problem (19) is feasible. Accordingly, the minimum thickness $h_{\min}$ is iteratively computed by applying the bisection method to an initial interval $[h_a, h_b]$ whose endpoints correspond to an unsafe and a safe thickness, respectively. Compared to other approaches available in the literature (see, e.g., reference [17]), the adopted procedure has the merit of circumventing unavoidably nonlinear optimization in the unknown minimum thickness and instead addressing a sequence of straightforward linear programming problems.
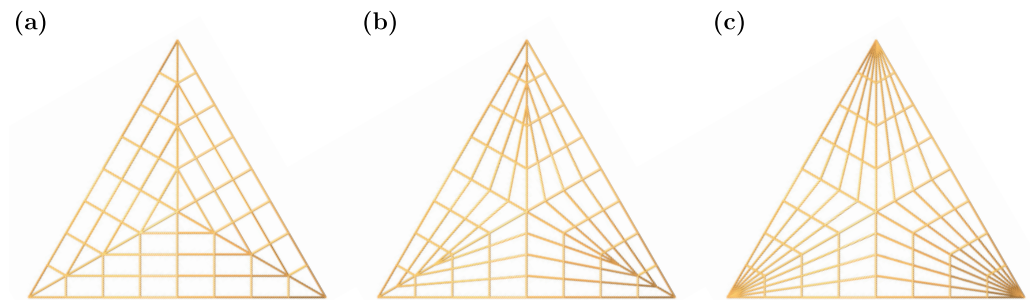
4. Structural Analysis of the Musmeci Vault Reinvented as a Masonry Structure

In this section, a masonry instance of the Musmeci vault is considered and its structural safety is investigated using GTNA.

For complying with the original geometry, the vault thickness is assumed to be the only design parameter. A uniform normalized thickness $h/2a = 0.02$ is initially considered, corresponding to a thickness $h = 25\,\text{cm}$. Outward horizontal settlements are considered in the rib planes at the corner supports for a minimum-thrust investigation.

To that end, the beam network topologies depicted in plan view in Figure 6 are adopted for the discretization of the vault mid-surface. The network refinement is controlled by a refinement parameter N, coinciding with the number of beams along the half-web (the case $N = 4$ is illustrated in the figure). Panels (a) and (c), respectively, refer to orthogonal and fan-like networks, obtained by adapting the form diagrams proposed for a classical TNA of cross vaults with a square layout in reference [17]. Distinct patterns of internal force flows underlie the two network topologies. In particular, the orthogonal topology presupposes that the self-weight of the webs is first conveyed to the ribs, which are then in charge of its transmission to the corner supports. Conversely, a direct flow of the self-weight of the webs toward the corner supports is envisaged within the fan-like topology. Motivated by the potential blending of the two internal force flow patterns, the orthogonal and fan-like topologies are conveniently interpreted as the two limit cases, respectively, corresponding to $\lambda = 0$ and $\lambda = 1$, of a continuous sequence of network topologies indexed

by a shape parameter $\lambda \in [0, 1]$. By way of example, panel (b) of Figure 6 shows the beam network for the choice $\lambda = 0.5$. Thanks to the problem symmetry, in numerical simulations, one-sixth of the vault is considered and suitable symmetry conditions are accounted for on the symmetry planes. At the corner support, additional static admissibility conditions are prescribed, requiring the line of action of the resultant constraint reaction to be contained within the springing section.
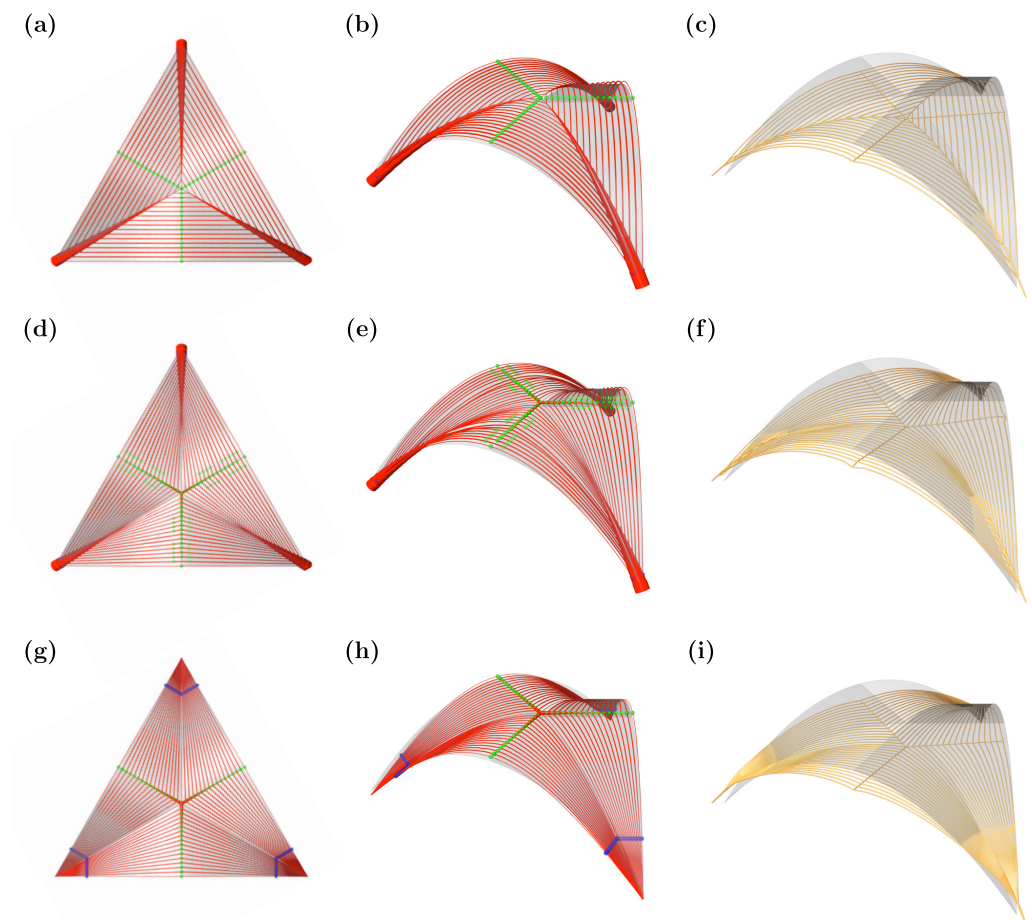

Figure 6. Structural analysis of the Musmeci vault reinvented as a masonry structure: beam networks in plan view. The network shape parameter is selected as (**a**) $\lambda = 0$, (**b**) $\lambda = 0.5$, and (**c**) $\lambda = 1$, with the former and latter cases identified as orthogonal and fan-like networks, respectively. Coarse networks are depicted for improved readability, corresponding to a network refinement parameter $N = 4$.

The left and mid columns of Figure 7 show the generalized thrust networks of minimum thrust for the Musmeci vault obtained assuming, from top to bottom, the values $\lambda = \{0, 0.5, 1\}$ for the network shape parameter. A refinement parameter $N = 16$ is considered. For the typical network beam b, a pipe with axis on the straight line $\tilde{r}^b$ and diameter proportional to $\tilde{N}^b$ (Section 3) is plotted. Green [resp., blue] dots are used to identify the beam end-sections where the generalized thrust network is tangent to the vault extrados [resp., intrados]. The orthogonal network prompts the formation of a series of web arches supported by the ribs, which thus play a fundamental static role (Figure 7a,b). Conversely, the fan-like network is characterized by the formation of fan arches, that interact on the vault ridge line, and directly rest on the corner supports (Figure 7g,h). An intermediate static regime is obtained for an intermediate value of the shape parameter, with the ribs that are only loaded in the regions close to the corner supports (Figure 7d,e). The right column of Figure 7 shows the settlement mechanisms of minimum thrust, which are kinematically dual to the obtained generalized thrust networks. A progressive transformation is recognized, from one driven by the settlement of the rib arches and triggering a settlement of the web arches for the orthogonal network, to one due to the settlement of the fan arches for the fan-like network. The obtained values of the normalized thrust are $H/V = \{1.039, 1.054, 1.079\}$ for $\lambda = \{0, 0.5, 1\}$, respectively. Accordingly, the orthogonal topology emerges as the most efficient pattern for the internal force flow.

The minimum thickness of the Musmeci vault reinvented as a masonry structure is then investigated. A vault is in minimum thickness configuration when the corresponding generalized thrust network is tangent to the vault extrados or intrados in a number of sections large enough that, from a kinematic viewpoint, the opening of the descending hinges implies an incipient collapse mechanism. By applying the procedure discussed in Section 3.4, the normalized minimum thickness is $h_{\min}/2a = 0.0105$, corresponding to a minimum thickness $h_{\min} \approx 13.1\,\text{cm}$ and a geometric safety factor $h/h_{\min} = 1.90$. The minimum thickness is attained using the orthogonal network topology and the relevant value of the normalized minimum thrust is $H/V = 1.120$. Such a result is in good agreement with the approximate estimate given in Equation (8) and follows from the similarity of the orthogonal internal force flow pattern with the one originally considered in the Musmeci model, where a generally compressive membrane stress state on the vault mid-surface is found. The present results are also in line with the predictions of 0.0112 and 1.116 for the normalized minimum thickness and the relevant normalized minimum thrust, respectively,

obtained using a slicing technique that generalizes the one adopted in the Musmeci model in order to avoid tensile stresses [3,4,8].

Figure 7. Structural analysis of the Musmeci vault reinvented as a masonry structure: generalized thrust network in (**left**) plan and (**mid**) perspective views, and (**right**) settlement mechanism of minimum thrust, assuming a uniform normalized thickness $h/2a = 0.02$. The network shape parameter is selected as (**a–c**) $\lambda = 0$, (**d–f**) $\lambda = 0.5$, and (**g–i**) $\lambda = 1$. The network refinement parameter is set to $N = 16$.

The small value obtained for its normalized minimum thickness proves the static efficiency of the cross vault geometry ideated by Musmeci. Although its unique design makes it difficult to compare with more conventional geometries, a qualitative clue can be achieved by considering a masonry cross vault with a square layout, a circular profile, and the same rise-to-span ratio ($f/2a = 0.292$) of the Musmeci vault as a benchmark. Its normalized minimum thickness is 0.0155, approximately 30% larger than the 0.0105 estimate previously obtained. Indeed, such a vault is characterized by a springing angle of about 30°, differing from the one of about 40° relevant to the original geometry. Nonetheless, upon referring to the larger class of masonry cross vaults with pointed circular profile investigated in references [17,19] for a benchmark, the normalized minimum thickness of such a vault with the same rise-to-span ratio and springing angle of the Musmeci one is 0.0111, which is still approximately 6% larger compared to the Musmeci geometry.

In closing, it is noticed that a further thickness reduction could be achieved by dropping off the assumption of uniform thickness. For instance, under the condition that the ribs are twice as thick as the webs, the normalized minimum thickness of the latter is 0.007, corresponding to a web thickness of 8.75 cm.

5. Parametric Analyses of Triangular Parabolic Masonry Cross Vaults

The Musmeci vault is here regarded as an instance of a class of triangular parabolic masonry cross vaults whose geometry is described by the rise-to-span ratio $f/2a$ and the uniform normalized thickness $h/2a$. The structural safety of such a class of vaults is thus investigated, accounting for their parameterized geometry.

As proposed in reference [17], the minimum and maximum thrusts are explored, resulting from outward or inward horizontal settlements in the rib planes at the corner supports, respectively. In Figure 8, the normalized thrust values, H_{min}/V and H_{max}/V are reported versus the normalized thickness $h/2a$, for the selected values $f/2a = \{0.2, 0.3, 0.5, 0.7, 1\}$ of the rise-to-span ratio. Red, yellow, and blue curves correspond to orthogonal ($\lambda = 0$), fan-like ($\lambda = 1$), and optimized ($\lambda = \lambda_{opt}$) beam networks, respectively. As expected, an increase in $f/2a$ implies a general decrease in the thrust regime, with the optimized network shape parameter shifting from $\lambda = 0$ to $\lambda = 1$ while considering vaults that are more and more slender. Moreover, an increase in $h/2a$ implies a larger interval $[H_{min}, H_{max}]$ of admissible thrusts for the vault, to be interpreted as an increase in the vault robustness.
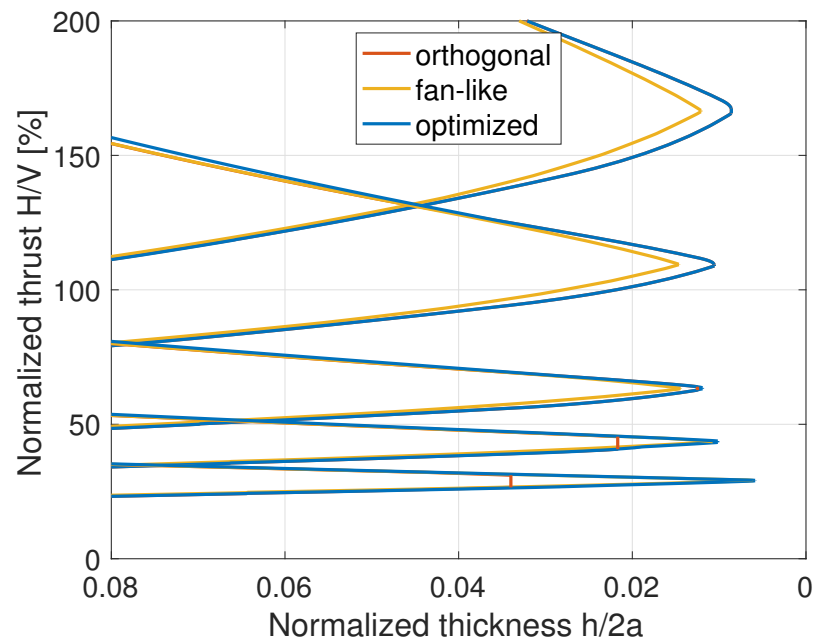
Figure 8. Parametric analyses of triangular parabolic masonry cross vaults: minimum/maximum normalized thrust H/V versus normalized thickness $h/2a$, for vaults with parabolic webs characterized by, from top to bottom, rise-over-span ratio $f/2a = \{0.2, 0.3, 0.5, 0.7, 1\}$. Orthogonal ($\lambda = 0$), fan-like ($\lambda = 1$), and optimized ($\lambda = \lambda_{opt}$) beam networks are considered.

A parametric analysis of the minimum thickness of the vault, with respect to the rise-to-span ratio $f/2a$, is then performed. The relevant results are shown in Figure 9, where the estimates obtained using the orthogonal, fan-like, and optimized networks of beams are compared. It is observed that the optimized minimum thickness versus rise-to-span ratio curve is characterized by two branches. The first [resp., second] branch, corresponding to shallow [resp., slender] vaults, is increasing [resp., decreasing] and attained with an orthogonal [resp., fan-like] network topology. The transition between the two branches takes place for vaults with intermediate values of $f/2a$ and requires intermediate values of the network shape parameter λ. In particular, a maximum of the curve is observed within such a connection branch, implying that the geometric safety factor of triangular parabolic masonry cross vaults under self-weight improves when considering shallow or slender geometries.
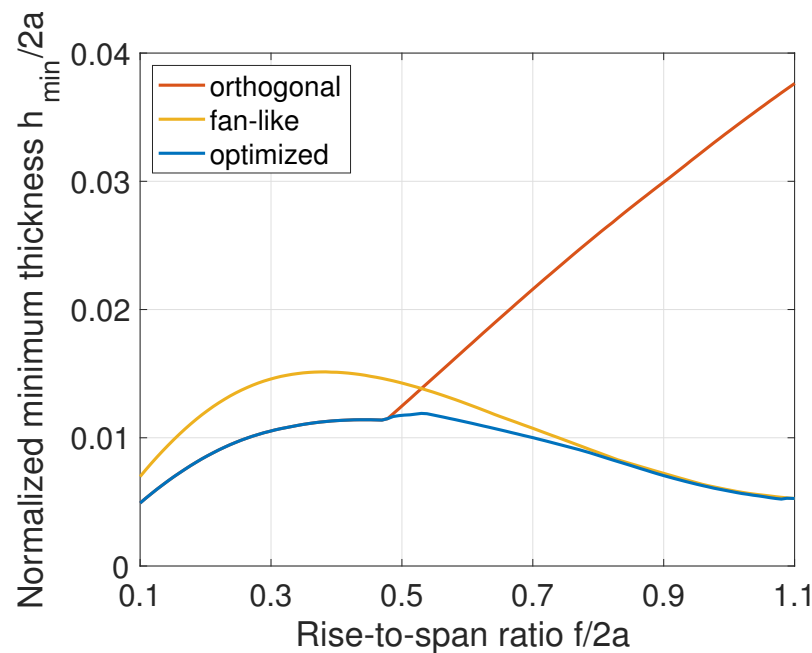
Figure 9. Parametric analyses of triangular parabolic masonry cross vaults: normalized minimum thickness $h_{\min}/2a$ versus rise-over-span ratio $f/2a$ for vaults with parabolic webs. Orthogonal ($\lambda = 0$), fan-like ($\lambda = 1$), and optimized ($\lambda = \lambda_{\text{opt}}$) beam networks are considered.

6. Conclusions

A triangular parabolic cross vault, that was designed by Musmeci in the 1950s to be realized as a reinforced concrete structure but remained unbuilt, has been revisited from the original perspective of its reinvention as a masonry structure. Relying on the classical Heyman's assumptions for masonry, the static theorem of limit analysis has been adopted as a structural analysis methodology, and its application through the recently proposed generalized thrust network analysis has been performed. In order to comply with the original geometry, the vault thickness has been first assumed as the only design parameter to conduct minimum-thrust and minimum-thickness analyses. A theoretical uniform thickness-to-span ratio of about 1% has been derived, showing the static efficiency of the unconventional geometry proposed by Musmeci. Then, assuming the vault rise-to-span ratio as a further design parameter, a more general class of triangular parabolic masonry cross vaults has been explored. It has been proven that, while shifting from shallow to slender geometries, a statically efficient internal force flow is obtained by progressively transforming a system of web arches that convey the self-weight loads to the ribs into a system of web arches that directly convey the self-weight loads to the corner supports. For especially shallow or slender geometries, extreme minimum thickness-to-span ratios appear to be conceivable. Ultimately, the obtained results prove the possibility of bringing new life to the smart Musmeci vault as a high-performance masonry structure.

Conflicts of Interest: The authors declare no conflict of interest.

References

1. Musmeci, S.; Vaccaro, G. Copertura a volte paraboliche per un mercato rurale. *L'Ingegnere* **1954**, *5*, 487–490.
2. Siegel, C. *Structure and Form in Modern Architecture*; Reinhold: New York, NY, USA, 1962.
3. Intrigila, C. Limit Analysis of Dry-Masonry Blocks Structures: Experimental and Numerical Investigation. Ph.D. Thesis, University of Rome Tor Vergata, Rome, Italy, 2020.
4. Intrigila, C.; Nodargi, N.A.; Bisegna, P. The unbuilt Musmeci parabolic cross vault reinvented as a dry-masonry structure. In Proceedings of the 12th International Conference on Structural Analysis of Historical Constructions (SAHC 2020), Barcelona, Spain, 16–18 September 2020; Roca, P., Molins, C., Pelà, L., Eds.; 2020. [CrossRef]
5. Heyman, J. The stone skeleton. *Int. J. Solids Struct.* **1966**, *2*, 249–279. [CrossRef]
6. Heyman, J. *The Stone Skeleton*; Cambridge University Press: Cambridge, UK, 1995. [CrossRef]
7. Como, M. *Statics of Historic Masonry Constructions*, 3rd ed.; Springer Series in Solid and Structural Mechanics; Springer International Publishing: Cham, Switzerland, 2017; Volume 9. [CrossRef]
8. Intrigila, C.; Nodargi, N.A.; Bisegna, P. Square Cross Vaults on Spreading Supports. In *Structural Analysis of Historical Constructions*; RILEM Bookseries; Aguilar, R., Torrealva, D., Moreira, S., Pando, M., Ramos, L.F., Eds.; Springer: Berlin/Heidelberg, Germany, 2019; Volume 18, pp. 1045–1053. [CrossRef]
9. O'Dwyer, D.W. Funicular analysis of masonry vaults. *Comput. Struct.* **1999**, *73*, 187–197. [CrossRef]
10. Block, P.; Ochsendorf, J. Thrust network analysis: A new methodology for three-dimensional equilibrium. *J. IASS* **2007**, *48*, 167–173.
11. Block, P.; Lachauer, L. Three-dimensional (3D) equilibrium analysis of gothic masonry vaults. *Int. J. Archit. Herit.* **2014**, *8*, 312–335. [CrossRef]
12. Block, P.; Lachauer, L. Three-dimensional funicular analysis of masonry vaults. *Mech. Res. Commun.* **2014**, *56*, 53–60. [CrossRef]
13. Fantin, M.; Ciblac, T. Extension of thrust network analysis with joints consideration and new equilibrium states. *Int. J. Space Struct.* **2016**, *31*, 190–202. [CrossRef]
14. Marmo, F.; Rosati, L. Reformulation and extension of the thrust network analysis. *Comput. Struct.* **2017**, *182*, 104–118. [CrossRef]
15. Bruggi, M. A constrained force density method for the funicular analysis and design of arches, domes and vaults. *Int. J. Solids Struct.* **2020**, *193–194*, 251–269. [CrossRef]
16. Maia Avelino, R.; Iannuzzo, A.; Van Mele, T.; Block, P. Assessing the safety of vaulted masonry structures using thrust network analysis. *Comput. Struct.* **2021**, *257*, 106647. [CrossRef]
17. Maia Avelino, R.; Iannuzzo, A.; Van Mele, T.; Block, P. Parametric Stability Analysis of Groin Vaults. *Appl. Sci.* **2021**, *11*, 3560. [CrossRef]
18. Block, P. Thrust Network Analysis: Exploring Three-Dimensional Equilibrium. Ph.D. Thesis, Massachusetts Institute of Technology, Cambridge, MA, USA, 2009.
19. Nodargi, N.A.; Bisegna, P. Generalized thrust network analysis for the safety assessment of vaulted masonry structures. *Eng. Struct. E* **2022**, *270*, 114878. [CrossRef]
20. Angelillo, M.; Fortunato, A. Equilibrium of masonry vaults. In *Novel Approaches in Civil Engineering*; Lecture Notes in Applied and Computational Mechanics; Frémond, M., Maceri, F., Eds.; Springer: Berlin/Heidelberg, Germany, 2004; Volume 14, pp. 105–111. [CrossRef]
21. Baratta, A.; Corbi, O. On the statics of No-Tension masonry-like vaults and shells: Solution domains, operative treatment and numerical validation. *Ann. Solid Struct. Mech.* **2011**, *2*, 107–122. [CrossRef]
22. Angelillo, M.; Babilio, E.; Fortunato, A. Singular stress fields for masonry-like vaults. *Continuum Mech. Thermodyn.* **2013**, *15*, 423–441. [CrossRef]
23. Montanino, A.; Olivieri, C.; Zuccaro, G.; Angelillo, M. From Stress to Shape: Equilibrium of Cloister and Cross Vaults. *Appl. Sci.* **2021**, *11*, 3846. [CrossRef]
24. Fraddosio, A.; Lepore, N.; Piccioni, M.D. Thrust surface method: An innovative approach for the three-dimensional lower bound limit analysis of masonry vaults. *Eng. Struct.* **2020**, *202*, 109846. [CrossRef]
25. Nodargi, N.A.; Bisegna, P. Minimum thrust and minimum thickness of spherical masonry domes: A semi-analytical approach. *Eur. J. Mech. A-Solids* **2021**, *87*, 104222. [CrossRef]
26. Nodargi, N.A.; Bisegna, P. A new computational framework for the minimum thrust analysis of axisymmetric masonry domes. *Eng. Struct.* **2021**, *234*, 111962. [CrossRef]
27. Nodargi, N.A.; Bisegna, P. Collapse capacity of masonry domes under horizontal loads: A static limit analysis approach. *Int. J. Mech. Sci.* **2021**, *212*, 106827. [CrossRef]
28. Nodargi, N.A.; Bisegna, P. A finite difference method for the static limit analysis of masonry domes under seismic loads. *Meccanica* 2021, *in press*. [CrossRef]
29. Milani, G. Simple lower bound limit analysis model for masonry double curvature structures. *Comput. Struct.* **2022**, *269*, 106831. [CrossRef]
30. Barsi, F.; Barsotti, R.; Bennati, S. Admissible shell internal forces and safety assessment of masonry domes. *Int. J. Solids Struct.* **2023**, *264*, 112082. [CrossRef]

31. Nodargi, N.A. An isogeometric collocation method for the static limit analysis of masonry domes under their self-weight. *Comput. Meth. Appl. Mech. Eng.* **2023**, *416*, 116375. [CrossRef]

32. D'Altri, A.M.; Sarhosis, V.; Milani, G.; Rots, J.; Cattari, S.; Lagomarsino, S.; Sacco, E.; Tralli, A.; Castellazzi, G.; de Miranda, S. Modeling Strategies for the Computational Analysis of Unreinforced Masonry Structures: Review and Classification. *Arch. Comput. Methods Eng.* **2020**, *27*, 1153–1185. [CrossRef]

33. Rossi, M.; Calderini, C.; Lagomarsino, S. Experimental testing of the seismic in-plane displacement capacity of masonry cross vaults through a scale model. *Bull. Earthq. Eng.* **2016**, *14*, 261–281. [CrossRef]

34. Foti, D.; Vacca, V.; Facchini, I. DEM modeling and experimental analysis of the static behavior of a dry-joints masonry cross vaults. *Constr. Build. Mater.* **2018**, *170*, 111–120. [CrossRef]

35. Chen, X.; Ou, W.; Chan, A.H.C.; Liu, H.; Fukuda, D. Vulnerability of pointed masonry barrel vaults subjected to differential settlement simulated with a GPGPU-Parallelized FDEM. *Int. J. Appl. Mech.* **2023**, *15*, 2350059. [CrossRef]